HHS Public Access

Author manuscript

Genes Brain Behav. Author manuscript; available in PMC 2021 April 09.

Published in final edited form as:

Genes Brain Behav. 2020 September ; 19(7): e12654. doi:10.1111/gbb.12654.

Phenotypic profiling of $mGlu_7$ knockout mice reveals new implications for neurodevelopmental disorders

Nicole M. Fisher[1,2], **Robert W. Gould**[1,2], **Rocco G. Gogliotti**[1,2], **Annalise J. McDonald**[1,2], **Hana Badivuku**[1,2], **Susmita Chennareddy**[1,2], **Aditi B. Buch**[1,2], **Annah M. Moore**[1], **Matthew T. Jenkins**[1,2], **W. Hudson Robb**[1,2], **Craig W. Lindsley**[1,2,3,4], **Carrie K. Jones**[1,2,5], **P. Jeffrey Conn**[1,2,4,5], **Colleen M. Niswender**[1,2,4,5]

[1]Department of Pharmacology, Vanderbilt University, Nashville, Tennessee

[2]Vanderbilt Center for Neuroscience Drug Discovery, Vanderbilt University, Nashville, Tennessee

[3]Department of Chemistry, Vanderbilt University, Nashville, Tennessee

[4]Vanderbilt Institute of Chemical Biology, Vanderbilt University, Nashville, Tennessee

[5]Vanderbilt Kennedy Center, Vanderbilt University Medical Center, Nashville, Tennessee

Abstract

Neurodevelopmental disorders are characterized by deficits in communication, cognition, attention, social behavior and/or motor control. Previous studies have pointed to the involvement of genes that regulate synaptic structure and function in the pathogenesis of these disorders. One such gene, *GRM7*, encodes the metabotropic glutamate receptor 7 ($mGlu_7$), a G protein-coupled receptor that regulates presynaptic neurotransmitter release. Mutations and polymorphisms in *GRM7* have been associated with neurodevelopmental disorders in clinical populations; however, limited preclinical studies have evaluated $mGlu_7$ in the context of this specific disease class. Here, we show that the absence of $mGlu_7$ in mice is sufficient to alter phenotypes within the domains of social behavior, associative learning, motor function, epilepsy and sleep. Moreover, *Grm7* knockout mice exhibit an attenuated response to amphetamine. These findings provide rationale for further investigation of $mGlu_7$ as a potential therapeutic target for neurodevelopmental disorders such as idiopathic autism, attention deficit hyperactivity disorder and Rett syndrome.

Keywords

ADHD; ASD; autism; EEG; epilepsy; *GRM7*; $mGlu_7$; Rett syndrome; seizures

Correspondence Colleen M. Niswender, Department of Pharmacology, Vanderbilt University, Nashville, TN 37232., colleen.niswender@vanderbilt.edu.
Present address: Robert W. Gould, Department of Physiology and Pharmacology, Wake Forest School of Medicine, Winston-Salem, North Carolina

CONFLICT OF INTEREST
The authors declare no potential conflict of interest.

SUPPORTING INFORMATION
Additional supporting information may be found online in the Supporting Information section at the end of this article.

1 | INTRODUCTION

Glutamate, the main excitatory neurotransmitter in the brain, acts by binding to ionotropic and metabotropic receptors expressed at synapses. The metabotropic glutamate receptors (*GRM*, mGlu receptors) are a class of G protein-coupled receptors (GPCRs) that modulate synaptic transmission and play important roles in both short- and long-term plasticity. The mGlu receptors are divided into three groups based on their sequence homology, G protein coupling and cellular localization: group I includes $mGlu_1$ and $mGlu_5$, group II includes $mGlu_2$ and $mGlu_3$, and group III includes $mGlu_4$, $mGlu_6$, $mGlu_7$ and $mGlu_8$.[1] Among the mGlu receptors, $mGlu_7$ is the most evolutionarily conserved and exhibits widespread expression across the mammalian brain.[2] $mGlu_7$ is expressed presynaptically on glutamatergic and GABAergic neurons and acts to inhibit neurotransmitter release both constitutively and in an activity-dependent manner.[3–5]

Emerging clinical evidence has associated the *GRM7* locus with neurodevelopmental disorders. For example, homozygous point mutations in *GRM7* have been reported in several patients with severe neurological diseases that are characterized by developmental delay and epilepsy,[6,7] while heterozygous mutations or deletions have been identified in patients with autism spectrum disorder (ASD)[8–10] and attention deficit hyperactivity disorder (ADHD).[11] Additionally, single-nucleotide polymorphisms have been associated with increased risk for ASD, ADHD and schizophrenia.[12–15]

We recently reported that $mGlu_7$ protein expression was significantly reduced in autopsy samples from patients with Rett syndrome (RTT),[16] suggesting that altered $mGlu_7$ expression can be a feature of monogenetic disorders in which the causative gene is not *GRM7*. In a mouse model of RTT, we found that potentiation of $mGlu_7$ activity with an allosteric modulator improved disease phenotypes.[16] This shows that $mGlu_7$ could be a feasible target for therapeutic intervention; however, these previous studies relied on a combination of nonselective compounds because a truly selective activator or positive allosteric modulator for $mGlu_7$ is not yet available. Therefore, more work is needed to validate $mGlu_7$ as a therapeutic target in RTT and to evaluate whether $mGlu_7$ potentiation can also provide benefit in other models of neurodevelopmental disorders.

$mGlu_7$ activity contributes to many behaviors in rodents that are implicated in neurodevelopmental disorders, such as cognition, mood and seizures (reviewed in 17); however, $mGlu_7$'s involvement in other areas, such as sociability, movement and sleep remain relatively unexplored. Therefore, we sought to investigate the contribution of $mGlu_7$ to phenotypic domains considered relevant to symptoms observed in neurodevelopmental disorders by characterizing $mGlu_7$ heterozygous (*Grm7*$^{+/-}$) and knockout (*Grm7*$^{-/-}$) mice of both sexes. In the current manuscript, we expand upon previously reported phenotypes, including cognitive deficits and seizures, and report novel phenotypic differences in social behavior, repetitive limb clasping, motor coordination, sleep–wake architecture and sensitivity to amphetamine. Together, these data show that $mGlu_7$ is well-positioned to modulate a wide range of behaviors that overlap with those that are characteristic of neurodevelopmental disorders in humans, and suggest that targeting $mGlu_7$ activity may be a novel treatment strategy for symptoms within these behavioral domains.

2 | METHODS

2.1 | Animals

All animals used in this study were group housed with food and water given ad libitum and maintained on a 12 hour light/dark cycle. Animals were cared for in accordance with the National Institutes of Health *Guide for the Care and Use of Laboratory Animals*. All studies were approved by the Institutional Animal Care and Use Committee for Vanderbilt University School of Medicine and took place during the light phase with the exception of EEG recordings. *Grm7* knockout mice were cryorecovered from the Mutant Mouse Regional Resource Center (B6.129P2-Grm7^{Tm1Dgen}/Mmnc). All mice were generated from heterozygous breeding pairs.

2.2 | Protein isolation and Western blotting

In experiments to measure c-Fos protein expression following generalized seizures, 30-week-old male mice were handled and tissue was collected 1 hour following seizure observation. Mice were anesthetized with isoflurane and decapitated. Tissue from the dorsal hippocampus, surrounding cortex and thalamus was dissected from a 1 mm coronal slice. Tissue samples were homogenized using a hand-held motorized mortar and pestle in radioimmunoprecipitation assay buffer (RIPA, Sigma). After homogenization, samples were spun for 20 minutes at 15 000g at 4°C. The supernatant was saved and protein concentration was determined using a bicinchoninic acid (BCA) protein assay (Pierce, Rockford, Illinois). Proteins (50 μg) were electrophoretically separated using a 4% to 20% SDS polyacrylamide gel and then transferred onto a nitrocellulose membrane (Bio-Rad, Hercules, California). Membranes were blocked with Odyssey blocking buffer (LiCor, Lincoln, Nebraska) for 1 hour at room temperature and probed with primary antibodies to c-Fos (1:1000, Millipore ABE457, Burlington, Massachusetts) and tubulin (1:5000, Abcam ab44928, Cambridge, Massachusetts) overnight at 4°C. Membranes were washed three times with Tris-buffered saline plus Tween 20 (25 mM Tris, 150 mM NaCl, 0.05% Tween 20) and then incubated with goat anti-rabbit fluorescent secondary antibody (800CW, 1:5000, LiCor) and goat anti-mouse fluorescent secondary antibody (680CW, 1:5000, LiCor). Blots were washed again and imaged with an Odyssey scanner and fluorescence was quantified using Image Studio Light software (LI-COR, Lincoln, Nebraska). Each value for c-Fos was normalized to the value calculated for tubulin.

2.3 | Long-term potentiation recordings

Coronal brain slices were prepared from 8- to 10-week-old mice. Mice were anesthetized with isoflurane and decapitated. Brains were rapidly removed and submerged in ice-cold sucrose cutting buffer containing: 230 mM sucrose, 2.5 mM KCl, 8 mM $MgSO_4$, 0.5 mM $CaCl_2$, 1.25 mM NaH_2PO_4, 10 mM glucose and 26 mM $NaHCO_3$ saturated with 95%/5% O_2/CO_2. A block of tissue containing hippocampus was trimmed, embedded in agarose and coronal slices 400 μm thick were cut using a Compresstome VF-200 (Precisionary Instruments, Greenville, North Carolina). Slices were transferred to a holding chamber containing *N*-methyl-D-glucamine (NMDG)-HEPES recovery solution (in mM, 93 NMDG, 2.5 KCl, 1.2 NaH_2PO_4, 30 $NaHCO_3$, 20 HEPES, 25 D-glucose, 5 sodium ascorbate, 2 thiourea, 3 sodium pyruvate, 10 $MgSO_4$, 0.5 $CaCl_2$, pH 7.3, 305 mOsm) for 15 minutes at

32°C. Slices were then transferred to room temperature artificial cerebral spinal fluid (ACSF) containing (in mM) 126 NaCl, 1.25 NaH_2PO_4, 2.5 KCl, 10 D-glucose, 26 $NaHCO_3$, 2 $CaCl_2$ and 1 $MgSO_4$, supplemented with 600 μM sodium ascorbate for at least 1 hour. Subsequently, slices were transferred to a submersion recording chamber and continuously perfused (2 mL/min) with ACSF heated to 30°C to 32°C. All solutions were continuously bubbled with 95%/5% O_2/CO_2.

A concentric bi-polar stimulating electrode was positioned near the CA3-CA1 border and paired-pulse field excitatory postsynaptic potentials (fEPSPs) were evoked (100 μs duration, every 20 seconds) and recorded with a glass electrode placed within the stratum radiatum of CA1. Input–output curves were generated for each slice and the stimulation intensity was adjusted to 50% of the maximum response for subsequent experiments. For long-term potentiation (LTP) experiments, slopes of three consecutive sweeps were averaged and normalized to the average slope during the baseline period. Data were digitized using a Multiclamp 700B, Digidata 1322A and pClamp 10 software (Molecular Devices, San Jose, California). LTP was induced by applying two trains of 100 Hz stimulation (high-frequency stimulation [HFS], 1 second duration, 20-second intertrain interval) after a 15 minute baseline. fEPSPs were monitored for 60 minutes after HFS and percent LTP was quantified as the average normalized slope during the last 5 minutes of recording.

2.4 | Phenotyping

Both male and female mice were used in phenotyping experiments. No significant sex differences were observed; therefore, data were combined. Mice underwent the following testing schedule with a minimum of 5 days of time between each test: open field (6 weeks), elevated plus maze (7 weeks), three-chamber social interaction (8 weeks), fear conditioning (9–10 weeks), motor assays (>10 weeks). A separate cohort of mice was used for the five-trial social recognition assay at 15 to 20 weeks of age. Limb clasping videos were taken at 5, 10, 15 and 20 weeks of age. For all tests, mice were habituated to the testing room for a minimum of 1 hour.

2.4.1 | Open field—Mice were placed in an activity chamber measuring 27 by 27 cm for 60 minutes where X, Y and Z beam breaks were monitored by Activity Monitor software (Med Associates, Inc., Fairfax, Vermont). The total distance traveled and time spent in the center of the chamber was quantified by this software.

2.4.2 | Elevated plus maze—Mice were placed on the elevated plus maze and allowed to explore freely for 5 minutes under full light. Time spent exploring each arm was measured using AnyMaze tracking software (Stoelting, Wood Dale, Illinois).

2.4.3 | Three-chamber social interaction—Mice were place in a three-chamber apparatus in which the test mouse was free to explore each chamber. Mice were habituated to the chamber for 5 minutes while two empty wire cups were present (phase 1). A novel mouse of the same strain and sex (stranger 1) was placed under one wire cup and the test mouse was left to explore freely for 7 minutes (phase 2). A second novel mouse of the same strain and sex from a different cage as stranger 1 (stranger 2) was then placed under the

remaining empty cup and the test mouse was allowed to explore for an additional 7 minutes (phase 3). The location of stranger 1 was alternated in a randomized fashion between test mice, but remained constant between phase 2 and phase 3 within each trial. The time spent in each chamber was quantified by AnyMaze tracking software.

2.4.4 | Five trial social recognition assay—Mice were placed in a 16 by 16 in. box with an empty wire cup placed in the center and allowed to habituate for 10 minutes. A novel mouse (stranger 1) of the same strain and sex was placed under the wire cup and a 2-minute trial was videotaped. Following a 10-minute interval, stranger 1 was introduced to the wire cup for another 2-minute trial. This was repeated for a total of four trials with stranger 1. For the fifth trial, a second novel mouse of the same strain and sex from a different cage as stranger 1 (stranger 2) was placed under the wire cup and a 2-minute trial was videotaped. For each trial, direct interaction of the test mouse with the wire cup was scored manually by a blinded observer.

2.4.5 | Fear conditioning—On training day, mice were placed into an operant chamber with a shock grid (Med Associates, Inc.) in the presence of a 10% vanilla odor cue. Following a 3-minute habituation period, two tone-shock pairings were administered consisting of a 30 second tone ending with a 1 second, 0.7 mA foot shock. Each tone-shock pairing was spaced 30 seconds apart and mice remained in the context for an additional 30 seconds after the second foot shock. On the next day, mice were tested for contextual fear memory by placing each animal back into the same chamber with a 10% vanilla odor cue for 3 minutes. Time spent freezing during a 3-minute testing period was quantified using Video Freeze software (Med Associates, Inc., Fairfax, Vermont). Four hours later, cued fear memory was assessed by placing the mice in a novel context (10% almond, no light). Following 1 minute of habituation in the novel context, the same auditory cue from conditioning was played for 1 minute. Freezing during each minute was quantified, and mice that froze >20% prior to the tone were excluded.

2.4.6 | Limb clasping—For each time point assessed, mice were suspended by the tail and video-recorded for 1 minute. Time spent clasping the fore and hindlimbs was quantified by a blinded scorer. For the forepaws, the timer was started when the paws were clearly clasped together and stopped when they were apart. The time was also counted when a noticeable repetitive “clapping” motion of the forepaws was observed. For the hindpaws, the timer was started when one or both hind limbs began to knuckle in, and the timer was stopped the paws came apart at any point. Time was counted if one paw remained knuckled in while the other came away. For both front and hind paws, the timer was stopped when the back of the mouse was turned to the camera.

2.4.7 | Gait analysis—Following a brief training session, mice were video-taped running at a speed of 18 cm/s on the Treadscan gait analysis system (CleverSys, Reston, Virginia). Discrete video clips of fluid gait were identified by the Treadscan software and manually checked by the experimenter. A foot model was built from *Grm7*$^{+/+}$ mice and used to process gait dynamics in accordance with the manufacturer’s instructions.

2.4.8 | Rotarod—Mice were placed on an accelerating rotarod (4–40 rpm over 3 minutes) and the latency to fall from the apparatus was recorded with a cut off of 180 seconds. Mice underwent three trials per day with a rest period of 30 to 60 minutes between each trial. Data from each day were averaged.

2.4.9 | Grip strength—Mice were suspended by the tail and allowed to place their forepaws on a wire grid angled at 45° and attached to a force transducer (SD Instruments, San Diego, California). Mice were then pulled by the tail until they let go of the apparatus and the maximal force was recorded. This assay was performed by two separate experimenters and the values for each mouse were averaged.

2.4.10 | Seizure evaluation—Mice were handled at least once weekly by being picked up by the tail and placed back into their home cage. Seizure severity was described using the Racine scale defined as: 1 = mouth and/or facial movements, increased digging; 2 = head nodding; 3 = forelimb clonus and tonic tail; 4 = rearing and/or tonic body; 5 = generalized seizure with motor convulsions.

2.5 | Electroencephalography

2.5.1 | Surgery—At 5 to 6 weeks of age, female *Grm7*$^{+/+}$ and *Grm7*$^{-/-}$ mice were surgically implanted under isoflurane anesthesia with a telemetric transmitter (HD-X02; Data Sciences International [DSI], Minneapolis, MN) for recording EEG, electromyography (EMG) and motor activity as previously described.[18–20] Transmitters were implanted subcutaneously just off the midline of the dorsal flank of each mouse under aseptic conditions. Transmitter leads were tunneled subcutaneously to the skull. Holes were drilled in the skull and exposed wires were placed directly in contact with the dura and secured via dental cement (Butler Schein, Henry Schein, Melville, New York). One lead was placed at +1 mm AP, −2 mm ML and the other was placed at −3 mm AP, +2 mm ML. An additional set of leads was placed bilaterally in the nuchal muscle for EMG recording. Animals were individually housed following surgery for the duration of the study and allowed to recover for a minimum of 1 week prior to the first EEG recording.

2.5.2 | Recordings—Uninterrupted EEG recordings occurred every 4 weeks between 8 and 20 weeks of age. Approximately 12 hours before each EEG study began, mice were moved into the recording room for habituation. EEG and EMG were recorded from the home cage of each animal continuously for 48 hours beginning at the onset of the light cycle on the day of each study. Telemetric EEG and EMG waveform data were collected using Ponemah software (DSI). Data were continuously sampled at a rate of 250 Hz and transmitted via a receiver (RPC-1; DSI) placed below the cage of each mouse to a computer for off-line analysis. For the amphetamine challenge, a 30-minute baseline EEG recording was obtained prior to subcutaneous administration of 2.25 mg/kg amphetamine (3 mg/kg amphetamine sulfate) followed by an additional 2.5 hours of EEG recording.

2.5.3 | Sleep staging and analysis—Trained observers, blinded to condition (age, genotype or pharmacological challenge) scored each 5-second epoch using Neuroscore 3.0 software (DSI, Minneapolis, Minnesota) to determine sleep/wake stages, including wake,

nonrapid eye movement (NREM) or rapid eye movement (REM) sleep based on accepted characteristic oscillatory patterns as previously published by our group.[18–20] The amount of time in each stage (wake, NREM, REM) during each 12-hour period (light, dark), along with bout numbers and duration, were quantified. Power spectra were computed in 1 Hz bins from 0.5 to 80 Hz using a Fast Fourier Transform with a Hamming window and overlap ratio of 0.5 for each mouse in 5-seconds epochs. Spectral power was examined across the entire spectrum within discrete states (eg, Wake, NREM or REM). We examined power within predefined frequency ranges (Delta [0.5–4 Hz], Theta [4–8 Hz], Alpha [8–13 Hz], Beta [13–30 Hz], Low Gamma [30–50 Hz] and High Gamma [50–80 Hz]) by averaging the power from all 5-second epochs within that state to yield the state-dependent relative power spectrum in either 12 hour light or 12 hour dark periods as previously described.[20] To examine effects of amphetamine on EEG, spectral power within the frequency bands defined above were averaged across the 30-minute baseline period; power during waking epochs only was then binned in 10-minute bins and expressed as a percent change from the 30-minute baseline. Activity counts were quantified and expressed in 10-minute bins.

2.6 | Statistical analysis

All data shown represent mean ± SEM. Statistical significance between groups was determined by an unpaired *t* test, paired *t* test or analysis of variance (ANOVA) with Bonferroni comparisons where appropriate. For each figure, the number of animals of each sex per group is indicated in the figure legend. In all cases, *P*-values are indicated as $*P < .05$, $**P < .01$, $***P < .001$, $****P < .0001$.

3 | RESULTS

3.1 | *Grm7*$^{-/-}$ and *Grm7*$^{+/-}$ mice exhibit abnormal social behavior

Social behavior is a major symptom domain disrupted in neurodevelopmental disease and a core diagnostic criterion for ASD. We tested social behavior in mice using a three-chamber interaction assay. *Grm7*$^{+/+}$, *Grm7*$^{+/-}$ and *Grm7*$^{-/-}$ littermates were placed in a three-chamber apparatus and allowed to explore freely. When given the choice to explore a novel mouse (stranger 1) or an empty cup, all genotypes preferred to interact with the mouse (Figure 1A, ANOVA, chamber: $F_{[2111]} = 76.6$, $P < .0001$, comparison of stranger 1 to empty: *Grm7*$^{+/+}$: $P = .0001$, *Grm7*$^{+/-}$: $P < .0001$, *Grm7*$^{-/-}$: $P < .0001$), suggesting that general sociability is unaffected in *Grm7*$^{-/-}$ mice. When given the choice to explore stranger 1 vs a second novel mouse (stranger 2), *Grm7*$^{+/+}$ and *Grm7*$^{+/-}$ mice showed a clear preference for stranger 2 (Figure 1B, ANOVA, chamber: $F_{(2,111)} = 47.7$, $P < .0001$, interaction: $F_{(4,111)} = 7.3$, $P < .0001$, comparison of stranger 1 to stranger 2: *Grm7*$^{+/+}$: $P = .0001$, *Grm7*$^{+/-}$: $P = .02$). However, *Grm7*$^{-/-}$ mice showed the opposite preference and spent significantly more time with stranger 1 (Figure 1B, *Grm7*$^{-/-}$: $P = .02$). When data were analyzed to only include close interaction time, a preference for stranger 1 over an empty cup was present for each genotype (Figure 1C, chamber: $F_{[1,74]} = 44.3$, $P < .0001$, comparison of stranger 1 to empty: *Grm7*$^{+/+}$: $P = .0005$, *Grm7*$^{+/-}$: $P = .0004$, *Grm7*$^{-/-}$: $P = .002$). A comparison of close interaction time between stranger 1 and stranger 2 showed a significant preference for stranger 2 in *Grm7*$^{+/+}$ controls only (Figure 1D, chamber: $F_{(1,74)} =$

4.1, $P = .046$, interaction: $F_{(2,74)} = 8.0$, $P = .0007$, comparison of stranger 1 to stranger 2: $Grm7^{+/+}$: $P = .006$).

To further test social recognition, a separate cohort of mice underwent a five-trial social recognition assay whereby each mouse was allowed to explore a novel mouse (stranger 1) for four 2-minute trials with 10 minutes between each trial. During the fifth trial, the test mouse was introduced to a second novel mouse (stranger 2). In this test, we observed no genotype differences in social interaction time across trials (Figure 1E, ANOVA, trial: $F_{(3.1,84.6)} = 17.9$, $P < .0001$, genotype: $F_{(2,27)}=0.4$, $P = .67$), and all genotypes showed a significantly increased interaction time between trial 4 and trial 5 (Figure 1F–H, paired t tests, $Grm7^{+/+}$: $t_{(9)}=2.8$, $P = .02$, $Grm7^{+/-}$: $t_{(10)}=2.8$, $P = .018$, $Grm7^{-/-}$: $t_{(8)}=4.2$, $P = .003$). Taken together, these data indicate that the loss of $mGlu_7$ does not affect general sociability or social recognition, but rather impacts social preference, motivation or other factors underlying social behavior.

To control for potential changes in spontaneous locomotor behavior, we tested mice in the open field assay and found no differences between groups (Figure S1A, ANOVA, $F_{(2,57)} = 0.24$, $P = .78$); however, $Grm7^{-/-}$ mice spent significantly more time in the center of the open field (Figure S1B, ANOVA, $F_{(2,57)} = 9.4$, $P = .0003$, $Grm7^{+/+}$ vs $Grm7^{-/-}$: $P = .03$), consistent with previously reports of diminished anxiety-like behavior in this model.[21] A similar phenotype was also observed in the elevated plus maze, whereby $Grm7^{-/-}$ mice spent significantly more time exploring the open arms of the maze (Figure S1C, ANOVA, $F_{[2,62]} = 6.0$, $P = .004$, $Grm7^{+/+}$ vs $Grm7^{-/-}$: $P = .012$).

3.2 | $Grm7^{-/-}$ mice have deficits in associative fear learning despite intact LTP in the hippocampus

Intellectual disability is a stand-alone diagnosis and a symptom domain that has high comorbidity with many neurodevelopmental disorders, including ASD,[22] To test associative learning, mice underwent a fear conditioning protocol that consisted of a 3-minute habituation to a novel context, followed by two mild foot shocks paired to an auditory cue. Consistent with previous findings showing that pain sensitivity is unaffected in $Grm7^{-/-}$ mice,[23] we did not observe changes in shock threshold (data not shown), suggesting that differences in foot shock sensitivity do not confound behavioral responses in this task. During this conditioning session, $Grm7^{+/+}$ and $Grm7^{+/-}$ mice progressively froze more after each foot shock, while $Grm7^{-/-}$ mice exhibited a markedly decreased freezing response (Figure 2A, ANOVA, shock: $F_{(2,219)} = 24.3$, $P < .0001$, interaction: $F_{(4,219)} = 4.8$, $P = .001$, $Grm7^{+/+}$ vs $Grm7^{-/-}$ shock 2: $P = .0004$). Twenty-four hours after conditioning, mice were placed back into the same context and freezing during a 3-minute session was quantified. $Grm7^{-/-}$ mice froze significantly less than their littermates (Figure 2B, ANOVA, $F_{[2,73]} = 22.8$, $P < .0001$, $Grm7^{+/+}$ vs $Grm7^{-/-}$: $P < .0001$). Four hours following the context test, mice were placed in a second novel context and the auditory cue was played. Again, $Grm7^{-/-}$ mice froze significantly less than their littermate controls (Figure 2C, ANOVA, $F_{(2,59)}=9.9$, $P = .0002$, $Grm7^{+/+}$ vs $Grm7^{-/-}$: $P = .025$).

Deficits in contextual fear learning can often be correlated with decreased synaptic plasticity within the hippocampus, as shown in rodent models of intellectual disability.[24,25]

Pharmacological inhibition of $mGlu_7$ activity can block LTP at Schaffer Collateral—CA1 (SC-CA1) synapses[26]; therefore, we tested the effect of $mGlu_7$ absence on this specific form of LTP. Following two trains of HFS, fEPSPs in hippocampal slices from *Grm7*$^{-/-}$ mice remained potentiated from baseline for 60 minutes (Figure 2D), and the magnitude of LTP, quantified during the last 5 minutes of recording, was not significantly different across genotypes (Figure 2E, ANOVA, $F_{(2,40)} = 2.1$, $P = .13$).

3.3 | *Grm7*$^{-/-}$ mice show a variety of deficits in motor coordination and strength

Motor stereotypies and impaired purposeful movement frequently occur in neurodevelopmental disorders; for example, repetitive hand wringing and gait abnormalities are core diagnostic criteria for RTT.[27] Although *Grm7*$^{-/-}$ mice did not differ in spontaneous locomotion as assessed in the open field (Figure S1A), they did exhibit motor abnormalities when challenged by paradigms that test strength and coordination. Upon weaning, we observed repetitive clasping of both the forepaws and hind paws in *Grm7*$^{-/-}$ mice when they were suspended by the tail. Clasping was captured on video and quantified by a blinded scorer at 5, 10, 15 and 20 weeks of age. Forepaw clasping in *Grm7*$^{-/-}$ mice was significantly increased at all ages and showed a significant interaction with age (Figure 3A, ANOVA, age: $F_{(3,148)} = 8.6$, $P < .0001$, genotype: $F_{(2,128)} = 123.1$, $P < .0001$, interaction: $F_{(6,148)} = 3.9$, $P = .01$, *Grm7*$^{+/+}$ vs *Grm7*$^{-/-}$ at all ages: $P < .001$). Hind paw clasping was significantly increased at all ages, but did not change significantly with age (Figure 3B, ANOVA, age: $F_{(3,148)} = 1.4$, $P = .25$, genotype: $F_{(2,128)} = 150.6$, $P < .0001$, *Grm7*$^{+/+}$ vs *Grm7*$^{-/-}$ at all ages: $P < .0001$). *Grm7*$^{-/-}$ mice also exhibited modest gait abnormalities when tested using a Treadscan system; specifically, the average swing and stride times of the front paws were significantly longer than littermate controls, while there was no difference in these parameters for the back paws between any group (Figure 3C, Swing: ANOVA, $F_{(2,33)} = 7.1$, $P = .003$, *Grm7*$^{+/+}$ vs *Grm7*$^{-/-}$: $P = .008$, stride: ANOVA, $F_{(2,33)} = 6.5$, $P = .004$, *Grm7*$^{+/+}$ vs *Grm7*$^{-/-}$: $P = .01$; back paw data not shown). In a rotarod test, *Grm7*$^{-/-}$ mice fell from the accelerating rod significantly sooner than their littermates (Figure 3D, ANOVA, day: $F_{(2,186)} = 17.3$, $P < .0001$, genotype: $F_{(2,186)} = 25$, $P < .0001$, *Grm7*$^{+/+}$ vs *Grm7*$^{-/-}$ day 2: $P = .02$, day 3: $P = .003$). This effect did not correlate with impairments in motor learning (Figure 3E, ANOVA, day: $F_{(2,186)} = 21.4$, $P < .0001$, genotype: $F_{(2,186)} = 0.034$, $P = .96$,) or differences in weight (Figure 3F, correlation, *Grm7*$^{+/+}$: $r = -.210$, *Grm7*$^{+/-}$: $r = .106$, *Grm7*$^{-/-}$: $r = .208$). *Grm7*$^{-/-}$ mice also exhibited reduced forepaw grip strength, which could contribute to their decreased latency to fall from the rotarod (Figure 3G, ANOVA, $F_{(2,37)} = 6.4$, $P = .004$, *Grm7*$^{+/+}$ vs *Grm7*$^{-/-}$: $P = .02$).

3.4 | Seizures in *Grm7*$^{-/-}$ mice can be induced by handling and involve hippocampal activation

Epilepsy is a common comorbidity in neurodevelopmental disorders that arises from excitatory/inhibitory imbalance that is often a result of deficits in synaptic development and function.[28] Over the course of testing, *Grm7*$^{-/-}$ mice and littermate controls were handled at least once per week, during which time we quantified the robust presence of behavioral seizures. These seizures were brief (<1 minute), ranged from a Racine score of 3 to 5, and were observed in 64% of *Grm7*$^{-/-}$ mice (9/14 mice by 20 weeks of age), with a median age of onset of 15 weeks of age and were never observed in *Grm7*$^{+/+}$ or *Grm7*$^{+/-}$ littermates

(Figure 4A). To evaluate the development of these seizures, a cohort of female *Grm7*$^{-/-}$ mice and *Grm7*$^{+/+}$ littermates was monitored by surface EEG from 8 to 20 weeks of age. No seizures were detectable during periods when the mice were left undisturbed; however, handling-induced generalized seizures were observed in 8/11 *Grm7*$^{-/-}$ mice and were detectable by EEG (Figure 4B). To further investigate which brain regions were involved in these seizures, we quantified c-Fos induction by Western blotting of protein isolated from brain tissue punches from the cortex, thalamus and hippocampus collected 1 hour following an observed seizure. Compared with *Grm7*$^{+/+}$ and *Grm7*$^{-/-}$ mice that did not experience a seizure, samples from *Grm7*$^{-/-}$ mice following a seizure showed a large increase in c-Fos only in the hippocampus (Figure 4C,D, ANOVA, cortex: $F_{(2,6)} = 1.9$, $P = .22$, hippocampus: $F_{(2,6)} = 15.0$, $P = .005$, *Grm7*$^{+/+}$ vs *Grm7*$^{-/-}$: $P = .009$, thalamus $F_{(2,6)} = 1.3$, $P = .34$). This suggests that seizures in *Grm7*$^{-/-}$ mice likely involve limbic regions; however, the contribution of other brain regions cannot be excluded as our study only captured one time point.

3.5 | EEG analysis of *Grm7*$^{-/-}$ mice indicate alterations in sleep and blunted response to amphetamine

In addition to epileptiform activity, EEG analysis also allowed for characterization of sleep–wake architecture, which is commonly disrupted in neurodevelopmental disorders.[29] *Grm7*$^{-/-}$ mice (blue bars) exhibited increased percent time awake during both the light phase (Figure 5A, ANOVA, time: $F_{(2.9,51.4)} = 8.9$, $P < .0001$, genotype: $F_{(1,18)}=9.5$, $P = .006$) and the dark phase (Figure 5B, ANOVA, genotype: $F_{(1,18)}=17.6$, $P = .0005$), along with decreased percent time in NREM sleep during both phases (Light phase: Figure 5C, time: $F_{(2.5,45.7)} = 12.8$, $P < .0001$, genotype: $F_{(1,18)}=6.0$, $P = .02$, Dark phase: Figure 5D ANOVA, genotype: $F_{(1,18)} = 20$, $P = .0003$, *Grm7*$^{+/+}$ vs *Grm7*$^{-/-}$: 16 weeks $P = .03$, 20 weeks $P = .03$). There was a significant effect of time, but not genotype, on percent time in REM sleep during the light phase (Figure 5E, ANOVA, time: $F_{(2.2,39)} = 4.0$, $P = .02$, genotype: $F_{(1,18)} = 0.007$, $P = .93$). Bout analysis of REM sleep showed a significant effect of time and genotype-time interaction on the number of bouts during the light phase (Figure 5G, ANOVA, time: $F_{(2.4,44)} = 8.4$, $P = .0004$, genotype: $F_{(1,18)} = 4.0$, $P = .06$, interaction: $F_{(3,54)} = 3.4$, $P = .02$). Average REM bout duration was significantly decreased during the light phase at 8 and 12 weeks of age (Figure 5H, ANOVA, time: $F_{(2.4,42.6)} = 3.2$, $P = .04$, genotype: $F_{(1,18)} = 16.1$, $P = .0008$, *Grm7*$^{+/+}$ vs *Grm7*$^{-/-}$: 8 weeks $P = .01$, 12 weeks $P = .004$).

Quantitative EEG (qEEG) analysis did not indicate consistent age-dependent or genotype-dependent changes in relative spectral power across widely accepted bands (eg, delta, theta, alpha; beta, gamma, Figure S2); therefore, we hypothesized that, similar to handling-induced seizures, differences may emerge following stimulation. We examined the effects of amphetamine on brain function in this cohort because *GRM7* polymorphisms have been associated with response to methylphenidate in ADHD patients.[30,31] Following a single dose, we observed a significantly reduced effect of amphetamine on activity counts in *Grm7*$^{-/-}$ mice (Figure 6A, ANOVA, time: $F_{(17,198)} = 15.9$, $P < .0001$, genotype: $F_{(1,198)} = 47.2$, $P < .0001$, interaction: $F_{(17,198)} = 4.5$, $P < .0001$, min 50: $P = .046$, min 60 to 90: $P < .0001$, min 100: $P = .036$). This was comorbid with a significantly blunted effect of

amphetamine on high gamma power (50–80 Hz) in *Grm7*$^{-/-}$ mice (Figure 6B, ANOVA, time: $F_{(17,185)} = 7.4$, $P < .0001$, genotype: $F_{(1,185)} = 16.1$, $P < .0001$, interaction: $F_{(17,185)} = 1.9$, $P = .02$, min 40: $P = .002$, min 50: $P = .02$) along with effects on low gamma power (30–50 Hz) (Figure 6C, ANOVA, time: $F_{(17,185)} = 2.7$, $P = .0004$, genotype: $F_{(1,185)} = 19.3$, $P < .0001$) and delta power (0.5–4 Hz) (Figure 6D, ANOVA, time: $F_{(17,185)} = 2.9$, $P = .0002$, genotype: $F_{(1,185)} = 67.0$, $P < .0001$, interaction: $F_{(17,185)} = 2.7$, $P = .0006$, min 40–80: $P < .01$). There were no significant changes in other frequency bands (Figure S3).

4 | DISCUSSION

Our data show a wide range of disrupted phenotypes in *Grm7*$^{-/-}$ mice, some of which replicate and expand upon published findings, while others have not been previously reported. A major novel finding is the disruption of social behavior in the three-chamber assay. Masugi-Tokita et al recently showed that $mGlu_7$ in the bed nucleus of the stria terminalis is essential for intermale aggression, and that male *Grm7*$^{-/-}$ mice show less frequent anogenital sniffing and more frequent grooming of an intruder.[32,33] In female mice, Gryksa et al showed that *Grm7*$^{-/-}$ animals exhibit decreased maternal aggression and increased maternal care.[34] Additionally, the $mGlu_7$ negative allosteric modulator (NAM) MMPIP was reported to decrease social interaction time in rats.[35] Our data suggest that loss of $mGlu_7$ also impairs social preference, motivation or another aspect of behavior in the three-chamber assay, but not the ability to recognize and interact with a new mouse. Both *Grm7*$^{-/-}$ and *Grm7*$^{+/-}$ mice exhibited a lack of preference when only close interaction was analyzed; interestingly, this is the only phenotype that we observed in heterozygous mice. As social deficits are a core symptom of ASD and common in other neurodevelopmental disorders, $mGlu_7$'s role in social behaviors and its underlying neural circuits merits further investigation.

The existing literature on *Grm7*$^{-/-}$ mice has focused primarily on anxiety, depression and emotional learning. Specifically, loss of $mGlu_7$ has been shown to produce phenotypes predictive of antidepressive and anxiolytic effects in rodent models,[21] and *Grm7*$^{-/-}$ mice have been characterized extensively in paradigms of fear and aversion learning in which they show a clear deficit.[23,36,37] Here, we corroborate these findings in a fear conditioning assay where we observed decreased associative memory in response to both context and cue. However, cued fear results should be interpreted with caution as variants in *GRM7* have been linked to age-related hearing loss in human populations,[38] and this association remains unstudied in mice.

LTP at SC-CA1 synapses is one form of synaptic plasticity that has been correlated with cognitive deficits across a range of neurological diseases, including neurodevelopmental disorders. $mGlu_7$ activation is required for LTP at SC-CA1 synapses through its ability to reduce GABAergic inhibition onto CA1 pyramidal cells.[26] Application of an $mGlu_7$ NAM can completely block LTP; however, a previous study reported no change in LTP at SC-CA1 synapses in *Grm7*$^{-/-}$ mice despite a significant decrease in potentiation directly following 100 Hz stimulation.[39] Our results confirm that LTP is not significantly altered by *Grm7* genotype, suggesting that compensatory mechanisms may occur with global deletion of $mGlu_7$.

To the best of our knowledge, the motor phenotypes we observed in *Grm7*$^{-/-}$ mice have not been previously published. Rotarod performance and grip strength were characterized in *Grm7*$^{-/-}$ mice at 8 to 10 weeks of age by Callaerts-Vegh et al[40]; in contrast, our testing was performed on animals that were greater than 10 weeks of age. Motor deficits in *Grm7*$^{-/-}$ mice may develop only at older ages and are likely aggravated by the onset of seizures. Only one time point was tested for rotarod, gait and grip strength; therefore, it will be important to investigate the developmental onset of these phenotypes in future studies. The repetitive clasping phenotype was apparent at 5 weeks of age and persisted through the entire testing period, indicating that at least some aspects of motor function are impacted early in life. Hindlimb clasping and gait abnormalities are commonly seen in many models of neurological disorders, including mouse models of RTT where it has been used widely as a measure of disease progression.[41] $mGlu_7$ is expressed on excitatory corticostriatal projections along with inhibitory striatopallidal and striatonigral projections[42]; however, the functional role of $mGlu_7$ in these circuits is poorly defined at present.

As $mGlu_7$ is a presynaptic regulator of glutamate release, its activation would be predicted to provide negative feedback in the event of high glutamate levels. Consistent with this idea, we routinely observed behavioral seizures in *Grm7*$^{-/-}$ mice. Spontaneous seizures in response to sensory stimuli, along with heightened excitability of area CA1 in hippocampal slices, has been previously reported.[43] Our data further support that these seizures involve the hippocampus and are only detectable following a stimulus, in this case, handling. Interestingly, the seizures we observed are very similar to those reported in mice lacking the protein Elfn1 (extracellular-leucine-rich repeat fibronectin domain 1), which were triggered by moving mice to a clean, empty cage and ranged on the Racine scale from a score of 2 to 5.[44,45] Elfn1 is a postsynaptic protein that promotes constitutive $mGlu_7$ activation and downstream inhibition of release probability onto somatostatin interneurons in the hippocampus and cortex.[5,46] The convulsive seizures observed in *Grm7*$^{-/-}$ and *Elfn1*$^{-/-}$ mice differ from those reported in mice after specific disruption of the interaction between $mGlu_7$ and Protein Interacting with C Kinase (PICK1). Disruption of the $mGlu_7$-PICK1 interaction leads to absence seizures that correlate with increased c-Fos expression with the thalamocortical circuit without changes in the hippocampus.[47] Constitutive activity of $mGlu_7$ provides tonic inhibition at thalamic synapses, an effect that is dependent on $mGlu_7$ interaction with PICK1.[48] Altogether, these data suggest that $mGlu_7$ may play distinct roles in seizure activity depending on seizure type, brain region involved and the expression of $mGlu_7$-interacting proteins. $mGlu_7$ activation would be predicted to reduce seizures, as shown by a recent report that the $mGlu_7$ agonist LSP2–9166 exhibits efficacy in two distinct models of chemically-induced epilepsy.[49]

We also report alterations in sleep architecture in female *Grm7*$^{-/-}$ mice assessed by EEG across time from 8 to 20 weeks of age. The balance of glutamate and GABA function is known to regulate sleep,[50] and normal sleep is critical for memory consolidation.[51] Reduced NREM sleep and altered REM bout patterns in *Grm7*$^{-/-}$ mice suggest abnormal sleep fragmentation, which has been specifically linked with deficits in contextual fear consolidation.[52] We did not observe any significant changes in qEEG spectra in *Grm7*$^{-/-}$ mice relative to their littermates when left undisturbed in their home cage. This is consistent with a previous publication that reported no differences in baseline qEEG but found

increased hippocampal theta power in *Grm7*$^{-/-}$ mice during a working memory task.[53] It is important to note that this EEG study was restricted to female mice because of interest in $mGlu_7$ as a potential target for Rett syndrome, where the relevant clinical population is predominantly female.

We also observed that *Grm7*$^{-/-}$ mice exhibited a significantly blunted response to amphetamine, which increased gamma power and lowered delta power in *Grm7*$^{+/+}$ animals. Oscillations in the gamma range are regulated by a balance in glutamate and GABA function,[54,55] evolve throughout development[56] and are thought to contribute to cognitive functions.[57] Amphetamines have been shown to strongly modulate gamma activity in attention-associated regions in adults with ADHD,[58] and, interestingly, there have been reports that polymorphisms in *GRM7* correlate with response to methylphenidate in ADHD patients.[30,31] We also observed a blunted effect of amphetamine on locomotor activity, which is consistent with the reported decrease in amphetamine-induced hyperlocomotion by the $mGlu_7$ NAM ADX71743.[59] These data could have implications for disease states such as ADHD and schizophrenia where abnormal dopaminergic signaling and aberrant gamma power is well established.[55,60] In further support of the $mGlu_7$-ELFN1 interaction, pathogenic mutations in the *ELFN1* gene have been identified in patients with ADHD and *Elfn1* knockout mice also have a reduced sensitivity to amphetamine.[44,45]

In summary, we report a wide range of altered phenotypes in *Grm7*$^{-/-}$ mice, many of which mirror those commonly observed in mouse models of neurodevelopmental disorders. We recently reported preclinical efficacy of $mGlu_7$ potentiation in a RTT mouse model.[16] One limitation of our previous work was the use of a nonselective compound that potentiates the activity of all group III mGlu receptors. The phenotypes reported here overlap extensively with those reported in RTT models (reviewed in 61), providing further support for $mGlu_7$ as a bona fide therapeutic target for RTT. Moreover, these data provide rationale for studying $mGlu_7$ in the context of neurodevelopmental disorders broadly and for investigating the therapeutic potential of compounds that increase $mGlu_7$ activity.

Supplementary Material

Refer to Web version on PubMed Central for supplementary material.

ACKNOWLEDGMENTS

This work was supported by NIMH R01 MH113543 (to C.M.N. and C. W.L.), NIMH R01 MH104158 (to C.M.N.) and CDMRP/DoD award W81XWH-17-1-0266 (to C.M.N.). N.M.F. was supported by NIH training grants T32 GM007628 and F31 MH113259. R.W.G. was supported by NIDA K99 grant DA042129. R.G.G. was supported by NIMH K01 MH112983 and a Young Investigator Award from the Brain Behavior Research Foundation (24970). The mouse strain used for this research project, B6.129P2-Grm7tm1Dgen/Mmnc, identification number 11626-UNC, was obtained from the Mutant Mouse Regional Resource Center, a NIH funded strain repository, and was donated to the MMRRC by Deltagen. Behavioral experiments were performed through use of the Vanderbilt Mouse Neurobehavioral Core.

Funding information Brain and Behavior Research Foundation, Grant/Award Number: 24970; Congressionally Directed Medical Research Programs, Grant/Award Number: W81XWH-17-1-0266; National Institute of General Medical Sciences, Grant/Award Number: T32 GM007628; National Institute of Mental Health, Grant/Award Numbers: F31 MH113259, K01 MH112983, R01 MH104158, R01 MH113543; National Institute on Drug Abuse, Grant/Award Number: DA042129

DATA AVAILABILITY STATEMENT

The data that support the findings of this study are available from the corresponding author upon reasonable request.

REFERENCES

1. Niswender CM, Conn PJ. Metabotropic glutamate receptors: physiology, pharmacology, and disease. Annu Rev Pharmacol Toxicol. 2010;50 (1):295–322. 10.1146/annurev.pharmtox.011008.145533. [PubMed: 20055706]
2. Flor PJ, Van Der Putten H, Rüegg D, et al. A novel splice variant of a metabotropic glutamate receptor, human mGluR7b. Neuropharmacology. 1997;36(2):153–159. 10.1016/S0028-3908(96)00176-1. [PubMed: 9144652]
3. Summa M, Di Prisco S, Grilli M, Usai C, Marchi M, Pittaluga A. Presynaptic mGlu7 receptors control GABA release in mouse hippocampus. Neuropharmacology. 2013;66:215–224. 10.1016/j.neuropharm.2012.04.020. [PubMed: 22564442]
4. Martín R, Torres M, Sánchez-Prieto J. mGluR7 inhibits glutamate release through a PKC-independent decrease in the activity of P/Q-type Ca^{2+} channels and by diminishing cAMP in hippocampal nerve terminals. Eur J Neurosci. 2007;26(2):312–322. 10.1111/j.1460-9568.2007.05660.x. [PubMed: 17650109]
5. Stachniak TJ, Sylwestrak EL, Scheiffele P, Hall BJ, Ghosh A. Elfn1-induced constitutive activation of mglur7 determines frequency-dependent recruitment of somatostatin interneurons. J Neurosci. 2019;39(23):4461–4474. 10.1523/JNEUROSCI.2276-18.2019. [PubMed: 30940718]
6. Charng W-L, Karaca E, Coban Akdemir Z, et al. Exome sequencing in mostly consanguineous Arab families with neurologic disease provides a high potential molecular diagnosis rate. BMC Med Genomics. 2016;9(1):42. 10.1186/s12920-016-0208-3. [PubMed: 27435318]
7. Reuter MS, Tawamie H, Buchert R, et al. Diagnostic yield and novel candidate genes by exome sequencing in 152 consanguineous families with neurodevelopmental disorders. JAMA Psychiat. 2017;74(3): 293–299. 10.1001/jamapsychiatry.2016.3798.
8. Gai X, Xie HM, Perin JC, et al. Rare structural variation of synapse and neurotransmission genes in autism. Mol Psychiatry. 2012;17(4):402–411. 10.1038/MP.2011.10. [PubMed: 21358714]
9. Sanders SJ, Murtha MT, Gupta AR, et al. De novo mutations revealed by whole-exome sequencing are strongly associated with autism. Nature. 2012;485(7397):237–241. 10.1038/nature10945. [PubMed: 22495306]
10. Liu Y, Zhang Y, Zhao D, et al. Rare de novo deletion of metabotropic glutamate receptor 7 (*GRM7*) gene in a patient with autism spectrum disorder. Am J Med Genet B Neuropsychiatr Genet. 2015;168(4):258–264. 10.1002/ajmg.b.32306.
11. Elia J, Glessner JT, Wang K, et al. Genome-wide copy number variation study associates metabotropic glutamate receptor gene networks with attention deficit hyperactivity disorder. Nat Genet. 2012; 44(1):78–84. 10.1038/ng.1013.
12. Yang Y, Pan C. Role of metabotropic glutamate receptor 7 in autism spectrum disorders: a pilot study. Life Sci. 2013;92(2):149–153. 10.1016/j.lfs.2012.11.010. [PubMed: 23201551]
13. Park S, Jung S-W, Kim B-N, et al. Association between the *GRM7* rs3792452 polymorphism and attention deficit hyperacitiveity disorder in a Korean sample. Behav Brain Funct. 2013;9(1):1. 10.1186/1744-9081-9-1. [PubMed: 23295062]
14. Ohtsuki T, Koga M, Ishiguro H, et al. A polymorphism of the metabotropic glutamate receptor mGluR7 (*GRM7*) gene is associated with schizophrenia. Schizophr Res. 2008;101(1–3):9–16. 10.1016/j.schres.2008.01.027. [PubMed: 18329248]
15. Noroozi R, Taheri M, Omrani MD, Ghafouri-Fard S. Glutamate receptor metabotropic 7 (*GRM7*) gene polymorphisms in mood disorders and attention deficit hyperactive disorder. Neurochem Int. 2019;129:104483. 10.1016/J.NEUINT.2019.104483. [PubMed: 31170425]
16. Gogliotti RG, Senter RK, Fisher NM, et al. mGlu 7 potentiation rescues cognitive, social, and respiratory phenotypes in a mouse model of Rett syndrome. Sci Transl Med. 2017;9(403):eaai7459. 10.1126/scitranslmed.aai7459. [PubMed: 28814546]

17. Fisher NM, Seto M, Lindsley CW, Niswender CM. Metabotropic glutamate receptor 7: a new therapeutic target in neurodevelopmental disorders. Front Mol Neurosci. 2018;11:387. 10.3389/fnmol.2018.00387. [PubMed: 30405350]
18. Gould RW, Nedelcovych MT, Gong X, et al. State-dependent alterations in sleep/wake architecture elicited by the M_4 PAM VU0467154—relation to antipsychotic-like drug effects. Neuropharmacology. 2016;102:244–253. 10.1016/j.neuropharm.2015.11.016. [PubMed: 26617071]
19. Rook JM, Xiang Z, Lv X, et al. Biased mGlu5-positive allosteric modulators provide in vivo efficacy without potentiating mGlu5 modulation of NMDAR currents. Neuron. 2015;86(4):1029–1040. 10.1016/j.neuron.2015.03.063. [PubMed: 25937172]
20. Nedelcovych MT, Gould RW, Zhan X, et al. A rodent model of traumatic stress induces lasting sleep and quantitative electroencephalographic disturbances. ACS Chem Neurosci. 2015;6(3):485–493. 10.1021/cn500342u. [PubMed: 25581551]
21. Cryan JF, Kelly PH, Neijt HC, Sansig G, Flor PJ, van der Putten H. Antidepressant and anxiolytic-like effects in mice lacking the group III metabotropic glutamate receptor mGluR7. Eur J Neurosci. 2003;17 (11):2409–2417. [PubMed: 12814372]
22. Christensen DL, Baio J, Braun KVN, et al. Prevalence and characteristics of autism spectrum disorder among children aged 8 years—autism and developmental disabilities monitoring network, 11 sites, United States, 2012. MMWR Surveill Summ. 2016;65(3):1–23. 10.15585/mmwr.ss6503a1.
23. Masugi M, Yokoi M, Shigemoto R, et al. Metabotropic glutamate receptor subtype 7 ablation causes deficit in fear response and conditioned taste aversion. J Neurosci. 1999;19(3):955–963. [PubMed: 9920659]
24. Jiang Y, Armstrong D, Albrecht U, et al. Mutation of the Angelman ubiquitin ligase in mice causes increased cytoplasmic p53 and deficits of contextual learning and long-term potentiation. Neuron. 1998;21(4):799–811. 10.1016/S0896-6273(00)80596-6. [PubMed: 9808466]
25. Moretti P, Levenson JM, Battaglia F, et al. Learning and memory and synaptic plasticity are impaired in a mouse model of Rett syndrome. J Neurosci. 2006;26(1):319–327. 10.1523/JNEUROSCI.2623-05.2006. [PubMed: 16399702]
26. Klar R, Walker AG, Ghose D, et al. Activation of metabotropic glutamate receptor 7 is required for induction of long-term potentiation at SC-CA1 synapses in the hippocampus. J Neurosci. 2015;35(19):7600–7615. 10.1523/JNEUROSCI.4543-14.2015. [PubMed: 25972184]
27. Neul JL, Kaufmann WE, Glaze DG, et al. Rett syndrome: revised diagnostic criteria and nomenclature. Ann Neurol. 2010;68(6):944–950. 10.1002/ana.22124. [PubMed: 21154482]
28. Bozzi Y, Casarosa S, Caleo M. Epilepsy as a neurodevelopmental disorder. Front Psych. 2012;3:19. 10.3389/fpsyt.2012.00019.
29. Robinson-Shelton A, Malow BA. Sleep disturbances in neurodevelopmental disorders. Curr Psychiatry Rep. 2016;18(1):6. 10.1007/s11920-015-0638-1. [PubMed: 26719309]
30. Mick E, Neale B, Middleton FA, McGough JJ, Faraone SV. Genome-wide association study of response to methylphenidate in 187 children with attention-deficit/hyperactivity disorder. Am J Med Genet B Neuropsychiatr Genet. 2008;147B(8):1412–1418. 10.1002/ajmg.b.30865. [PubMed: 18821564]
31. Park S, Kim B-N, Cho S-C, et al. The metabotropic glutamate receptor subtype 7 rs3792452 polymorphism is associated with the response to methylphenidate in children with attention-deficit/hyperactivity disorder. J Child Adolesc Psychopharmacol. 2014;24(4):223–227. 10.1089/cap.2013.0079. [PubMed: 24815731]
32. Masugi-Tokita M, Flor PJ, Kawata M. Metabotropic glutamate receptor subtype 7 in the bed nucleus of the stria terminalis is essential for Intermale aggression. Neuropsychopharmacology. 2016;41(3):726–735. 10.1038/npp.2015.198. [PubMed: 26149357]
33. Masugi-Tokita M, Yoshida T, Kageyama S, Kawata M, Kawauchi A. Metabotropic glutamate receptor subtype 7 has critical roles in regulation of the endocrine system and social behaviours. J Neuroendocrinol. 2018;30(3):e12575. 10.1111/jne.12575. [PubMed: 29377390]

34. Gryksa K, Mittmann L, Bauer A, et al. Metabotropic glutamate receptor subtype 7 controls maternal care, maternal motivation and maternal aggression in mice. Genes Brain Behav. 2019;19(1):e12627. 10.1111/gbb.12627. [PubMed: 31793148]
35. Hikichi H, Murai T, Okuda S, et al. Effects of a novel metabotropic glutamate receptor 7 negative allosteric modulator, 6-(4-methoxyphenyl)-5-methyl-3-pyridin-4-ylisoxazonolo[4,5-c]pyridin4(5H)-one (MMPIP), on the central nervous system in rodents. Eur J Pharmacol. 2010;639(1–3):106–114. 10.1016/j.ejphar.2009.08.047. [PubMed: 20371227]
36. Goddyn H, Callaerts-Vegh Z, Stroobants S, et al. Deficits in acquisition and extinction of conditioned responses in mGluR7 knockout mice. Neurobiol Learn Mem. 2008;90(1):103–111. 10.1016/J.NLM.2008.01.001. [PubMed: 18289889]
37. Goddyn H, Callaerts-Vegh Z, D'Hooge R. Functional dissociation of group III metabotropic glutamate receptors revealed by direct comparison between the behavioral profiles of knockout mouse lines. Int J Neuropsychopharmacol. 2015;18(11):pyv053. 10.1093/ijnp/pyv053. [PubMed: 25999589]
38. Friedman RA, Van Laer L, Huentelman MJ, et al. GRM7 variants confer susceptibility to age-related hearing impairment. Hum Mol Genet. 2009;18(4):785–796. 10.1093/hmg/ddn402. [PubMed: 19047183]
39. Bushell TJ, Sansig G, Collett VJ, van der Putten H, Collingridge GL. Altered short-term synaptic plasticity in mice lacking the metabotropic glutamate receptor mGlu7. Sci World J. 2002;2:730–737. 10.1100/tsw.2002.146.
40. Callaerts-Vegh Z, Beckers T, Ball SM, et al. Concomitant deficits in working memory and fear extinction are functionally dissociated from reduced anxiety in metabotropic glutamate receptor 7-deficient mice. J Neurosci. 2006;26(24):6573–6582. 10.1523/JNEUROSCI.1497-06.2006. [PubMed: 16775145]
41. Gogliotti RG, Senter RK, Rook JM, et al. mGlu5 positive allosteric modulation normalizes synaptic plasticity defects and motor phenotypes in a mouse model of Rett syndrome. Hum Mol Genet. 2016;25 (10):1990–2004. 10.1093/hmg/ddw074. [PubMed: 26936821]
42. Kosinski CM, Risso Bradley S, Conn PJ, et al. Localization of metabotropic glutamate receptor 7 mRNA and mGluR7a protein in the rat basal ganglia. J Comp Neurol. 1999;415(2):266–284. [PubMed: 10545164]
43. Sansig G, Bushell TJ, Clarke VR, et al. Increased seizure susceptibility in mice lacking metabotropic glutamate receptor 7. J Neurosci. 2001; 21(22):8734–8745. [PubMed: 11698585]
44. Dolan J, Mitchell KJ. Mutation of Elfn1 in mice causes seizures and hyperactivity. PLoS One. 2013;8(11):e80491. 10.1371/journal.pone.0080491. [PubMed: 24312227]
45. Tomioka NH, Yasuda H, Miyamoto H, et al. Elfn1 recruits presynaptic mGluR7 in trans and its loss results in seizures. Nat Commun. 2014;5(1):4501. 10.1038/ncomms5501. [PubMed: 25047565]
46. Sylwestrak EL, Ghosh A. Elfn1 regulates target-specific release probability at CA1-interneuron synapses. Science. 2012;338(6106):536–540. 10.1126/science.1222482. [PubMed: 23042292]
47. Bertaso F, Zhang C, Scheschonka A, et al. PICK1 uncoupling from mGluR7a causes absence-like seizures. Nat Neurosci. 2008;11(8):940–948. 10.1038/nn.2142. [PubMed: 18641645]
48. Tassin V, Girard B, Chotte A, et al. Phasic and tonic mGlu7 receptor activity modulates the thalamocortical network. Front Neural Circuits. 2016;10:31. 10.3389/fncir.2016.00031. [PubMed: 27199672]
49. Girard B, Tuduri P, Moreno MP, et al. The mGlu7 receptor provides protective effects against epileptogenesis and epileptic seizures. Neurobiol Dis. 2019;129:13–28. 10.1016/j.nbd.2019.04.016. [PubMed: 31051234]
50. Luppi P-H, Gervasoni D, Verret L, et al. Paradoxical (REM) sleep genesis: the switch from an aminergic–cholinergic to a GABAergic–glutamatergic hypothesis. J Physiol. 2006;100(5–6):271–283. 10.1016/j.jphysparis.2007.05.006.
51. Rasch B, Born J. About sleep's role in memory. Physiol Rev. 2013;93 (2):681–766. 10.1152/physrev.00032.2012. [PubMed: 23589831]

52. Lee ML, Katsuyama ÂM, Duge LS, et al. Fragmentation of rapid eye movement and nonrapid eye movement sleep without total sleep loss impairs hippocampus-dependent fear memory consolidation. Sleep. 2016;39(11):2021–2031. 10.5665/sleep.6236. [PubMed: 27568801]

53. Holscher C, Schmid S, Pilz PKD, Sansig G, van der Putten H, Plappert CF. Lack of the metabotropic glutamate receptor subtype 7 selectively modulates theta rhythm and working memory. Learn Mem. 2005;12(5):450–455. 10.1101/lm.98305. [PubMed: 16204199]

54. Fort P, Bassetti CL, Luppi P-H. Alternating vigilance states: new insights regarding neuronal networks and mechanisms. Eur J Neurosci. 2009;29(9):1741–1753. 10.1111/j.1460-9568.2009.06722.x. [PubMed: 19473229]

55. Gonzalez-Burgos G, Hashimoto T, Lewis DA. Alterations of cortical GABA neurons and network oscillations in schizophrenia. Curr Psychiatry Rep. 2010;12(4):335–344. 10.1007/s11920-010-0124-8. [PubMed: 20556669]

56. Le Van Quyen M, Khalilov I, Ben-Ari Y. The dark side of high-frequency oscillations in the developing brain. Trends Neurosci. 2006; 29(7):419–427. 10.1016/j.tins.2006.06.001. [PubMed: 16793147]

57. Benchenane K, Tiesinga PH, Battaglia FP. Oscillations in the prefrontal cortex: a gateway to memory and attention. Curr Opin Neurobiol. 2011;21(3):475–485. 10.1016/j.conb.2011.01.004. [PubMed: 21429736]

58. Franzen JD, Wilson TW. Amphetamines modulate prefrontal γ oscillations during attention processing. Neuroreport. 2012;23(12):731–735. 10.1097/WNR.0b013e328356bb59. [PubMed: 22776904]

59. Kalinichev M, Rouillier M, Girard F, et al. ADX71743, a potent and selective negative allosteric modulator of metabotropic glutamate receptor 7: in vitro and in vivo characterization. J Pharmacol Exp Ther. 2013;344(3):624–636. 10.1124/jpet.112.200915. [PubMed: 23257312]

60. Klein MO, Battagello DS, Cardoso AR, Hauser DN, Bittencourt JC, Correa RG. Dopamine: functions, signaling, and association with neurological diseases. Cell Mol Neurobiol. 2019;39(1):31–59. 10.1007/s10571-018-0632-3. [PubMed: 30446950]

61. Katz DM, Berger-Sweeney JE, Eubanks JH, et al. Preclinical research in Rett syndrome: setting the foundation for translational success. Dis Model Mech. 2012;5(6):733–745. 10.1242/dmm.011007. [PubMed: 23115203]

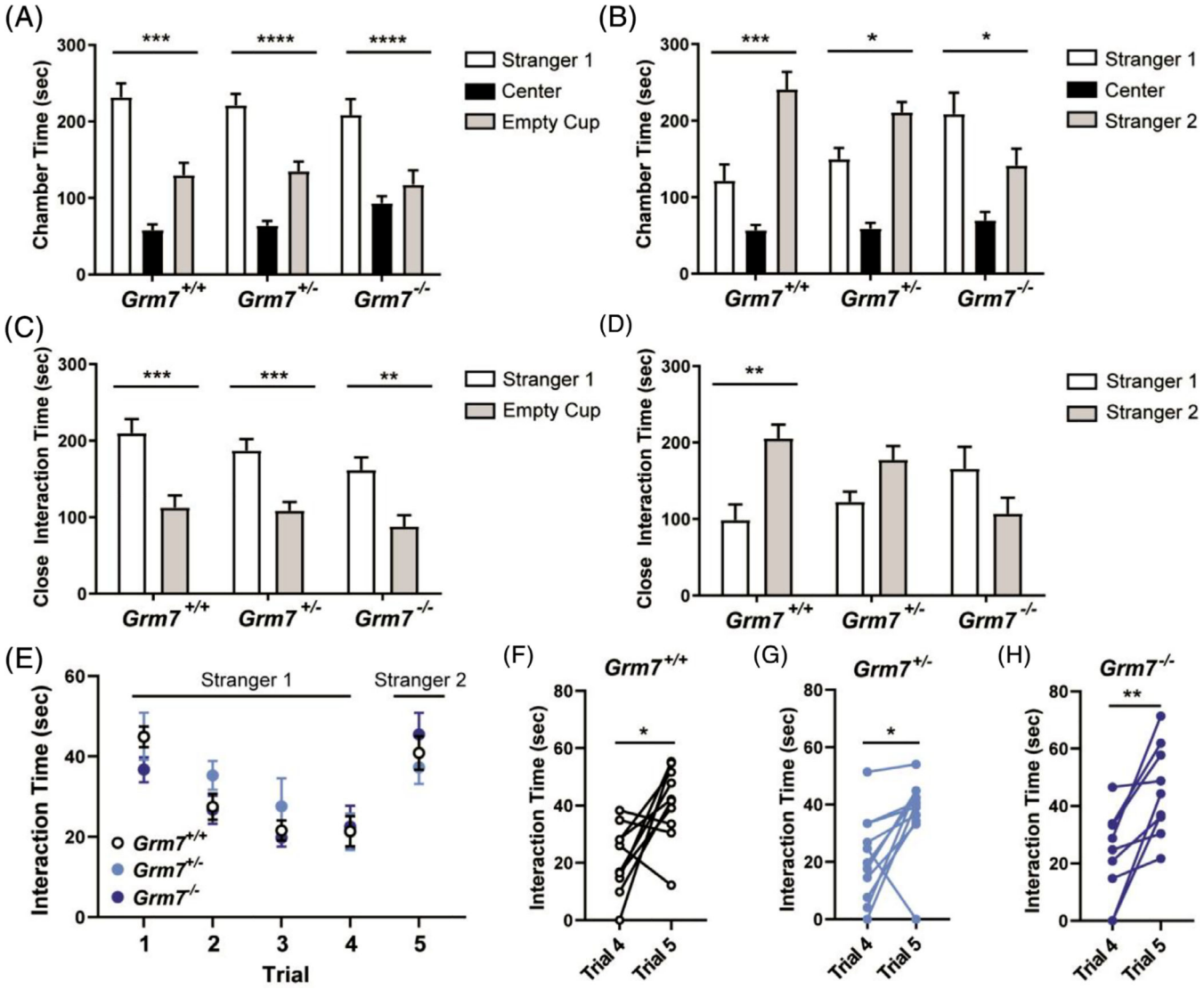

FIGURE 1.

Grm7$^{-/-}$ and *Grm7*$^{+/-}$ mice exhibit abnormal social behavior. A, Quantification of time in the chamber with stranger 1 relative to the chamber with the empty cup. B, Quantification of time in the chamber with stranger 2 relative to the chamber with stranger 1. C, Quantification of close interaction time with stranger 1 and empty cup. D, Quantification of close interaction time with stranger 1 and stranger 2. For panels (A) to (D), N = 10 *Grm7*$^{+/+}$ (6 female, 4 male), 15 *Grm7*$^{+/-}$ (10 female, 6 male), 14 *Grm7*$^{-/-}$ (8 female, 6 male). E, Five-trial social recognition assay. Quantification of interaction time over all trials. F–H, Paired t tests for each genotype comparing trial 4 and trial 5. For panels (E) to (H), N = 10 *Grm7*$^{+/+}$ (5 female, 5 male), 11 *Grm7*$^{+/-}$ (5 female, 6 male), 9 *Grm7*$^{-/-}$ (5 female, 4 male). **P* < .05, ***P* < .01, ****P* < .001, *****P* < .0001

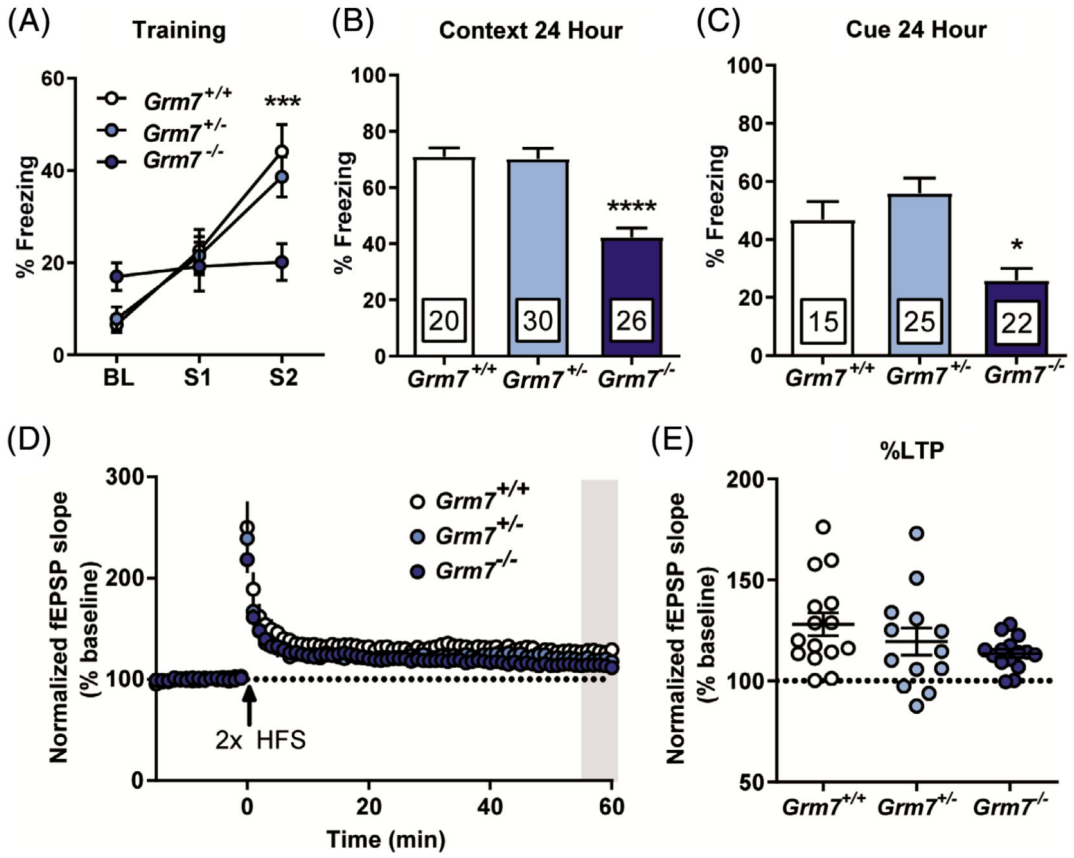

FIGURE 2.

Grm7$^{-/-}$ mice have deficits in associative fear learning despite intact long-term potentiation at SC-CA1 synapses. A, Quantification of acute freezing during baseline (BL) and in response to foot shocks (S1 and S2) during fear conditioning. B, Quantification of freezing behavior upon re-exposure to the conditioning context 24 hours postconditioning. For (A) and (B), N = 20 *Grm7*$^{+/+}$ (11 female, 9 male), 30 *Grm7*$^{+/-}$ (16 female, 14 male), 26 *Grm7*$^{-/-}$ (15 female, 11 male). C, Quantification of freezing behavior in response to a 1-minute auditory cue 4 hours after the context test. N = 15 *Grm7*$^{+/+}$ (9 female, 6 male), 25 *Grm7*$^{+/-}$ (13 female, 12 male), 22 *Grm7*$^{-/-}$ (12 female, 10 male). Five *Grm7*$^{+/+}$, five *Grm7*$^{+/-}$ and four *Grm7*$^{-/-}$ animals were excluded because of freezing >20% prior to the tone. D, Long-term potentiation at SC-CA1 synapses induced by two trains of high frequency stimulation (HFS, 100 Hz). N (total slices/total mice) = 15/9 *Grm7*$^{+/+}$ (10/6 female, 5/3 male), 13/8 *Grm7*$^{+/-}$ (6/4 female, 7/4 male), 15/8 *Grm7*$^{-/-}$ (8/4 female, 7/4 male). E, Quantification of LTP magnitude during the last 5 minutes of recording (gray bar in D). *$P < .05$, ***$P < .001$, ****$P < .0001$

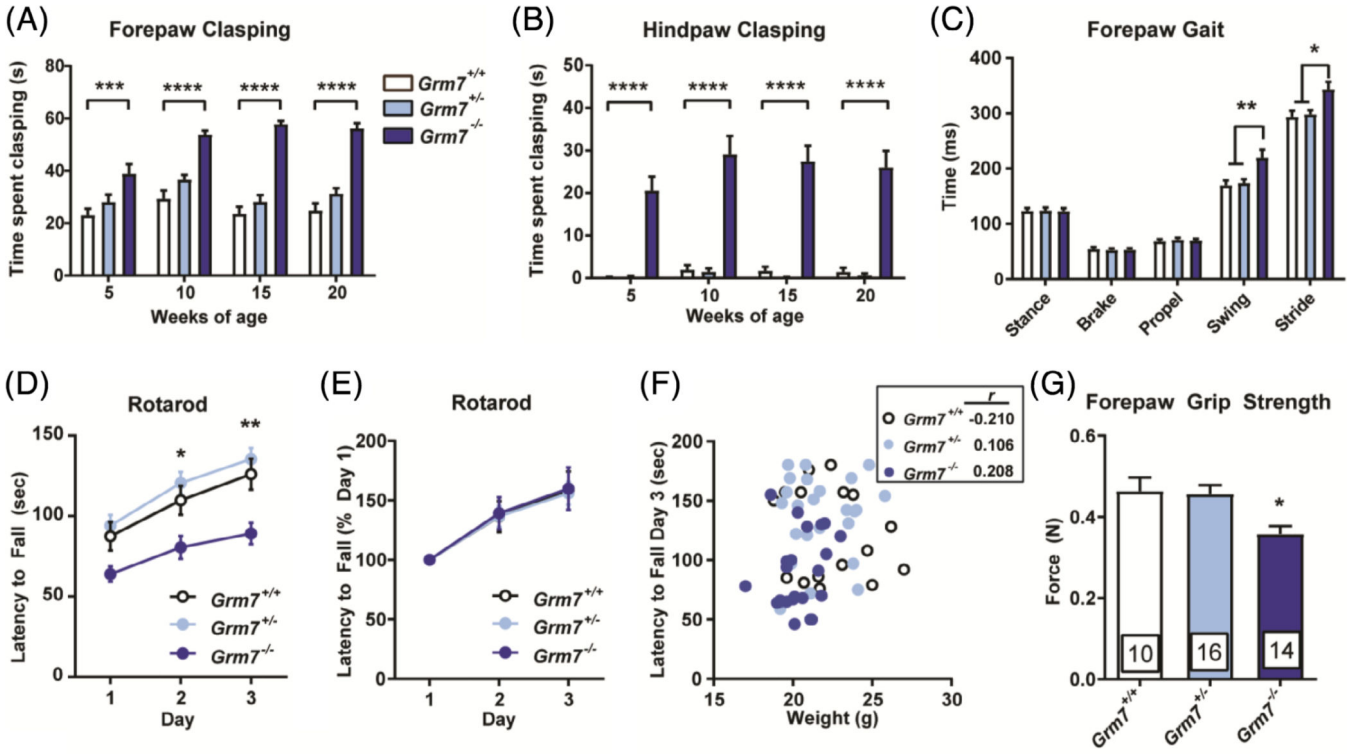

FIGURE 3.

Grm7$^{-/-}$ mice exhibit repetitive paw clasping along with deficits in motor coordination and strength. Quantification of forepaw, A, and hindpaw, B, clasping over time. N = 10 *Grm7*$^{+/+}$ (6 female, 4 male), 15 *Grm7*$^{+/-}$ (10 female, 6 male), 14 *Grm7*$^{-/-}$ (8 female, 6 male). C, Forepaw gait parameters measured by Treadscan system. N = 10 *Grm7*$^{+/+}$ (5 female, 5 male), 14 *Grm7*$^{+/-}$ (5 female, 9 male), 12 *Grm7*$^{-/-}$ (7 female, 5 male). D, Latency to fall from an accelerating rotarod over 3 days. E, Latency to fall from rotarod normalized to day 1. F, Lack of correlation of latency to fall from rotarod on day 3 with weight. *r* values shown in inset. For panels (D) to (F), N = 17 *Grm7*$^{+/+}$ (9 female, 8 male), 25 *Grm7*$^{+/-}$ (15 female, 10 male), 24 *Grm7*$^{-/-}$ (13 female, 11 male). G, Quantification of forepaw grip strength. N = 10 *Grm7*$^{+/+}$ (6 female, 4 male), 15 *Grm7*$^{+/-}$ (10 female, 6 male), 14 *Grm7*$^{-/-}$ (8 female, 6 male). **P* < .05, ***P* < .01, ****P* < .001, *****P* < .0001

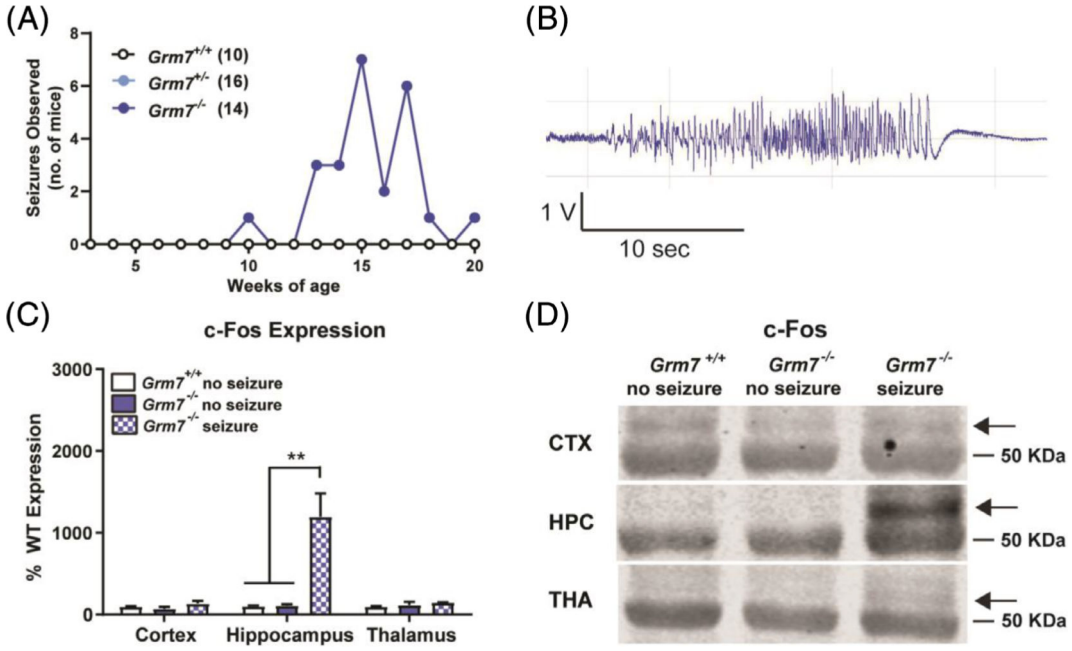

FIGURE 4.

Seizures in *Grm7*$^{-/-}$ mice correlate with increased c-Fos expression in the hippocampus. A, Seizure observations over time, including seizures with Racine score greater or equal to 3. N = 10 *Grm7*$^{+/+}$ (6 female, 4 male), 15 *Grm7*$^{+/-}$ (10 female, 6 male), 14 *Grm7*$^{-/-}$ (8 female, 6 male). B, Representative EEG trace of a seizure induced upon handling. C, Quantification of c-Fos protein by Western blot in tissue samples collected 1 hour following handling. Regions analyzed: cortex (CTX), hippocampus (HPC), thalamus (THA). N = 3 male mice per group, 30 weeks of age. D, Representative c-Fos blot photos. The arrow represents the band quantified in (C). The band below is a nonspecific band that aligns with the 50 kDa ladder marker

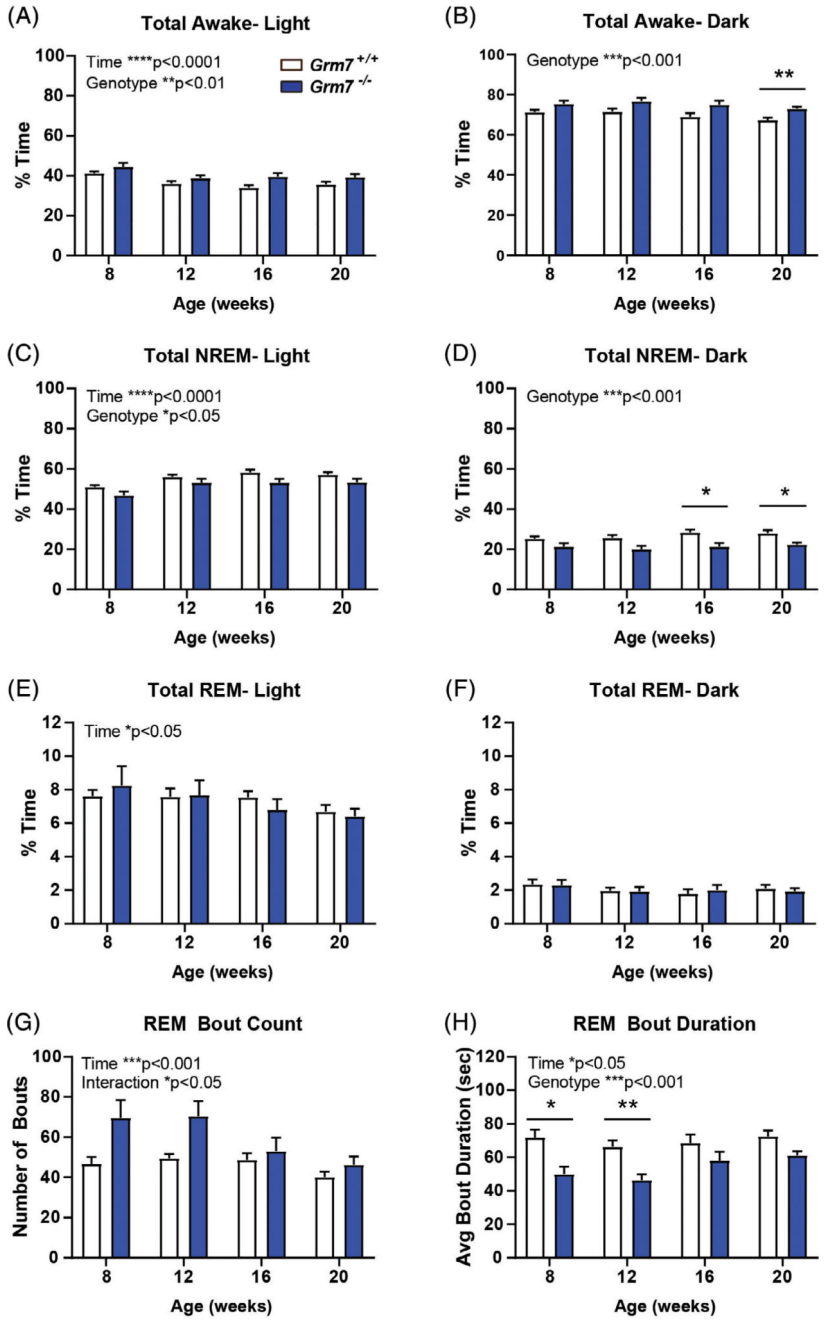

FIGURE 5.

Grm7$^{-/-}$ mice exhibit altered sleep–wake architecture. A, B, Percent of time spent awake during, A, light and, B, dark phases. C, D, Percent of time spent in NREM sleep during, C, light and, D, dark phases. E, F, Percent of time spent in REM sleep during, E, light and, F, dark phases. G, REM bout count and, H, bout duration during the light phase. For all panels, N = 9 female *Grm7*$^{+/+}$, 11 female *Grm7*$^{-/-}$. *P < .05, **P < .01, ***P < .001, ****P < .0001

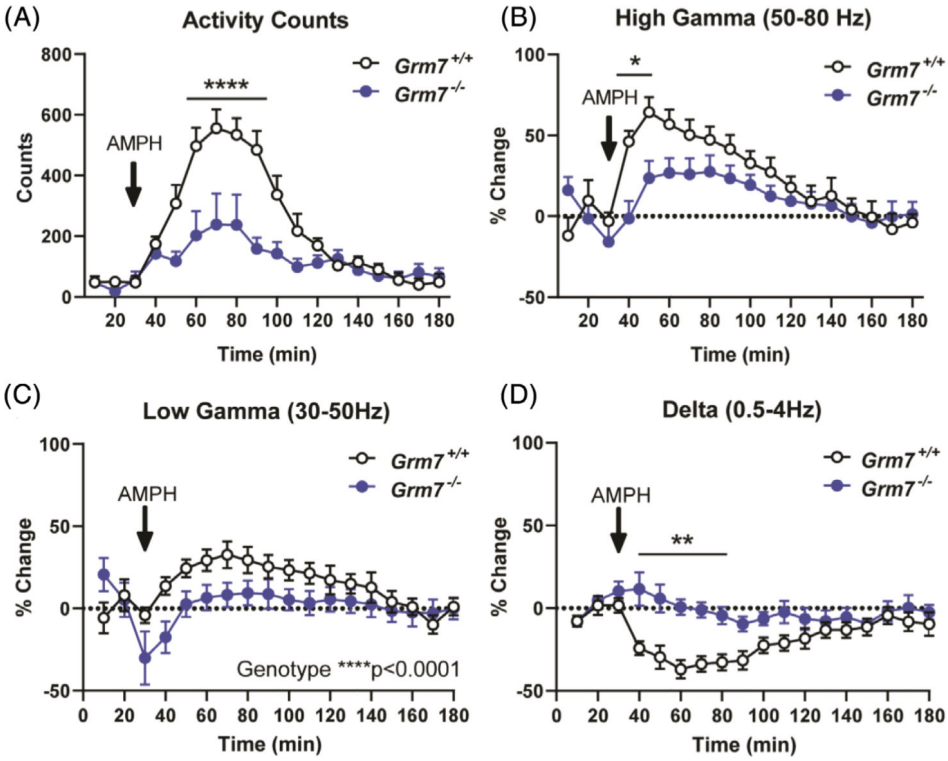

FIGURE 6.

The response to amphetamine is blunted in *Grm7*$^{-/-}$ mice compared with controls. Quantification of, A, activity counts, B, high gamma power, C, low gamma power and D, delta power following subcutaneous administration of 2.25 mg/kg amphetamine. For all panels, N = 6 female *Grm7*$^{+/+}$, 7 female *Grm7*$^{-/-}$. *$P < .05$, **$P < .01$, ****$P < .0001$